

## Size-Selective Shell Cross-Linked Interior Functionalized Siloxane Nanocages

Young-Woong Suh,<sup>†</sup> Mayfair C. Kung,<sup>†</sup> Yingmin Wang,<sup>‡</sup> and Harold H. Kung\*<sup>†</sup>

Department of Chemical and Biological Engineering, and Department of Materials Science and Engineering,  
Northwestern University, Evanston, Illinois 60208-3120

Received October 18, 2005; E-mail: hkung@northwestern.edu

Shell cross-linked micellar assemblies derived from diblock copolymers are well-known stable structures.<sup>1</sup> These structures, ranging from about 10 nm to micrometer in size, possess an amphiphilic core-shell morphology with intramicellar covalent cross-linking of the chain segments that comprise the micelle shell. They have found use in various applications, such as a template for mineralization,<sup>2</sup> a nanoreactor for the preparation and carrier of metallic catalysts,<sup>3</sup> and for controlled drug release.<sup>4</sup> Nanosize hollow particles (nanocages) derived from shell cross-linked micelle (SCM) templates are also known. They can be prepared by cleaving the core segment of the polymer using techniques, such as ozonization<sup>5</sup> or photochemical degradation.<sup>6</sup> Other techniques to synthesize structures containing cavities in this size range include sonochemistry,<sup>7</sup> use of organic or inorganic templates, such as liposome<sup>8</sup> or silica nanospheres,<sup>9</sup> onto which the shell is deposited, and polymerization of liposomes.<sup>10,11</sup>

Molecular-size nanocapsules can be made by self-assembly of, for example, pyrogalloarenes<sup>12</sup> or metal-catecholamide complexes.<sup>13</sup> To our knowledge, however, there are no reports for preparing hollow SCM particles, 2–5 nm in size, with an atomic-layer-thick, covalently linked, porous shell. The cavity of such a particle is of molecular dimension. If these particles also possess chemically and/or catalytically active groups covalently anchored in the interior, their cavities could function as robust nanosize reactors for controlled chemical processes. Furthermore, the cross-linked, porous shell would limit access into the cavity and could provide molecular size-selectivity, similar in concept to using end-group-functionalized dendrimers<sup>14</sup> or shape-selectivity in a molecular sieve. Here, we report a successful preparation of such a siloxane nanocage, derived from SCM, that possesses amine functional groups tethered to the inside surface of the shell.

The strategy is shown schematically in Figure 1. The concept is to generate nanometer-size micelles with template surfactants which contain headgroups that can be polymerized into a porous, cross-linked shell and hydrophobic tails that can be converted to a functional group afterward. The surfactant molecule used is (triethoxysilyl)propylcetylcarbamate **I**.<sup>15</sup> The hydrophobic tail of **I** contains a carbamate group that can be converted to an amine group. These molecules form micelles **II** in ethanol (step i), which is stable for days, as indicated by DLS (Supporting Information, SI), possibly due to hydrogen bonding between carbamate groups and between carbamate and ethoxy groups, as well as van der Waals interactions between alkyl chains in the tail. The hydrodynamic diameter of the micelles is about 2 nm (polydispersity 0.36), consistent with the length of the hydrocarbon tail. The siloxy headgroups, hydrolyzed to silanol with an ethanol-water mixture containing HCl, subsequently condense to form cross links. Further cross-linking is by reacting the remaining silanol groups with dimethyldimethoxysilane, and the remnant silanols are capped with

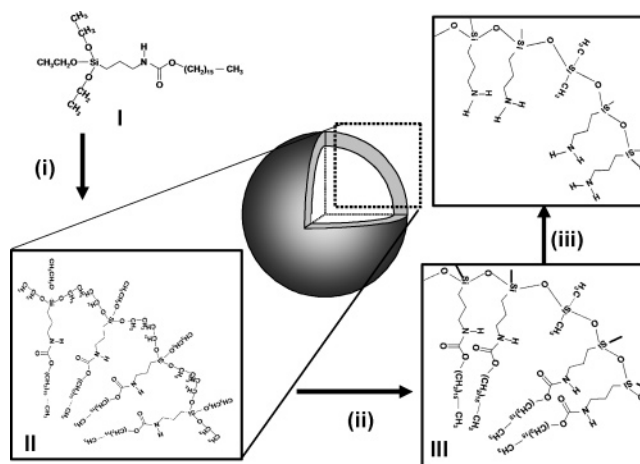


**Figure 1.** Schematic drawing showing the steps in the synthesis of a siloxane nanocage **IV**, containing propylamine groups tethered to the interior surface of an atomic-layer-thick, cross-linked siloxane shell, derived from the micelle of (triethoxysilyl)propylcetylcarbamate **I**. The inserts for **III** and **IV** are 2-D cutout representations of the cross-linked shell.

trimethylmethoxysilane to form SCM **III** (step ii). The transformations in these reactions are quantitative, as indicated by <sup>1</sup>H NMR (SI). The <sup>1</sup>H signals of ethoxysilyl disappeared completely at the completion of step ii, and ethanol was formed. **III** is soluble in ethanol and retains the 2 nm size (polydispersity 0.19). Interestingly, upon changing solvent from ethanol to a more hydrophobic mixture of ethanol/toluene (1:1), the cross-linked **III** is robust and retains its structure, whereas micelle **II**, without cross-linking, disintegrates.

The final shell cross-linked nanocage **IV** is generated by treatment of **III** with trimethyliodosilane to effect cleavage of the carbamate bond, followed by addition of methanol and purification (step iii) to form tethered amines. Since the hydrophobic hydrocarbon tails in **III** are interior to the siloxane shell, the silylpropylamine groups generated would be tethered to the interior surface of the shell in **IV**, as depicted schematically in Figure 1. Successful conversion of carbamate to amine is confirmed by <sup>1</sup>H NMR. From the peak areas at 4.01 ppm due to carbamate (OCOCH<sub>2</sub>) and 2.34 ppm due to aminopropyl (CH<sub>2</sub>N), it was estimated that 85% of the carbamate in **IV** was converted to amine. Presumably, the remaining carbamate groups are inaccessible, hidden in some sterically hindered sites. <sup>29</sup>Si NMR of **IV** in CDCl<sub>3</sub> showed a very weak signal at -18.335 ppm (reference TMS), which is a typical value for -O-Si(CH<sub>3</sub>)<sub>2</sub>-O-. The weak signal is likely due to slow tumbling of **IV** in solution because of its size. MALDI-TOF MS detected mass at 2560 and some smaller ones that differ from each other by a mass of 210–212. A range of sizes is expected due to our method of preparation. It is interesting to note that the mass of a O-Si-(CH<sub>3</sub>)<sub>2</sub>-O-Si(O)<sub>2</sub>(CH<sub>2</sub>CH<sub>2</sub>CH<sub>2</sub>NH<sub>2</sub>) unit is 208 and is 212 if the amine and all terminal siloxy groups are protonated by the matrix material ( $\alpha$ -cyano-4-hydroxycinnamic acid) used in MALDI-TOF

<sup>†</sup> Department of Chemical and Biological Engineering.

<sup>‡</sup> Department of Materials Science and Engineering.

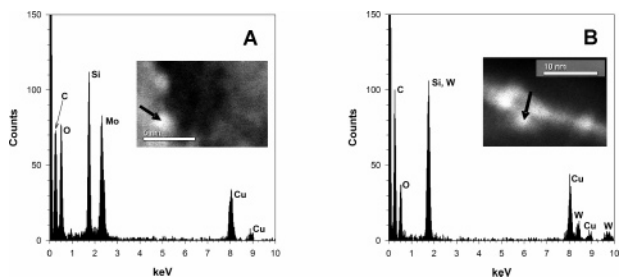


**Figure 2.** Z-contrast high-resolution electron micrographs and single particle EDX spectra of molybdate- (A) and tungstate-stained (B) **IV**, indicated by arrow in the insert, supported on carbon grid.

measurements. Thus, the distribution of masses supports the picture that **IV** is made of aminopropylsiloxy units cross-linked with methylsiloxy units. Since the acidic matrix material in the sample preparation for MALDI-TOF measurements causes cleavage of siloxane bonds, it is not possible to determine the molecular weight distribution. The highest mass detected of 2560 corresponds to about 12 disiloxane units, consistent with an estimate of about nine surfactant molecules in a 2 nm micelle.

That **IV** retains the size of **III** is confirmed by DLS (2 nm, polydispersity 0.37). Its spherical morphology is confirmed by TEM images (Figure 2) of **IV**, stained with aqueous solutions of ammonium molybdate (3 wt %) or ammonium tungstate (1 wt %), and the single particle EDX analyses. Individual particles, roughly 2 nm in diameter and spherical in shape, containing both Si and Mo or Si and W were observed. These elements were not detected in the background at a point 200–300 nm away from the particles. These observations strongly suggest that **IV** consists of an atomic or nearly atomic layer thick shell; otherwise, it would be larger in size.

The classical ninhydrin (2,2-dihydroxy-1,3-indandione) test was used to probe the amine groups in **IV**.<sup>16</sup> Exposing **IV** to ninhydrin in an ethanol solution followed by treatment with methanol results in the formation of Ruhemann's blue, which exhibits an intense blue color with an absorption maximum at 576 nm (SI). As a control experiment, exposure of ninhydrin to (aminopropyl)triethoxysilane (APTES) also generates a deep blue solution with the same absorption maximum. From the absorbance at 576 nm, it can be estimated that 85% of the starting silylcarbamate is converted to the silylpropylamine, which is in agreement with estimation from the NMR spectra.

Because the triethoxysilyl headgroup in the surfactant is much larger than the silanol group formed by hydrolysis, the resulting cross-linked shell in **IV** is quite porous and could offer molecular size-selectivity. The latter can be illustrated by comparing the ability of the amine groups to interact with molecules of different sizes, such as the smaller ninhydrin versus the larger Zn tetraphenylporphyrin (ZnTPP). ZnTPP forms a red solution in dichloromethane that exhibits an absorption maximum at 418 nm. It coordinates readily to sterically unhindered amines, such as APTES, to form a green complex with the absorption maximum shifted by 8 nm to 426 nm. On the other hand, although **IV** interacts readily with ninhydrin, there is no indication that it interacts with ZnTPP, and its presence did not shift the absorption maximum of the porphyrin (SI).

The amine groups in **IV** are catalytically active. They catalyze the decomposition of 3-oxobutanoic acid (acetoacetic acid) to CO<sub>2</sub> and acetone, which can react further to form dimethoxypropane in a methanol solution.<sup>17</sup> At room temperature, APTES (amine/reactant

ratio of 1/22.8) catalyzes the reaction with a turnover frequency of 0.7 mol (mol NH<sub>2</sub>·h)<sup>-1</sup> and a selectivity predominantly for acetone (88 and 86% at 10 and 27% conversion, respectively), consistent with acetone being the primary product. In contrast, for the amine groups in **IV** (amine/reactant molar ratio of 1/35), the turnover frequency is 4.4 mol (mol amine·h)<sup>-1</sup>, and the product selectivity favors acetal (57, 65, and 68% acetal at 12, 22, and 35% conversion, respectively). The results suggest that, in the nanocage, molecules are concentrated due to positive interaction with the siloxane shell, such as hydrogen bonding between carbonyl and amine and van der Waals interaction. The higher concentration of the reactant results in higher activity, and the longer residence time of the product acetone near the amine is consistent with the higher selectivity for the secondary product dimethoxypropane. This is a manifestation of confinement effect in a small cavity.

The synthesis strategy reported here permits variations of the size of the cavity and opening in the shell, as well as the nature of the tethered functional group by changing the length of the hydrophobic tail, and the nature of the hydrophilic headgroup and of the tail–headgroup linker of the surfactant. They will be investigated.

**Acknowledgment.** Financial support was from the U.S. Department of Energy, Basic Energy Science, Department of Science. J. Henao assisted in collecting MALDI-TOF data. Y.W.S. acknowledges fellowship support by Korea Research Foundation Grant funded by the Korean Government (MOEHRD, Basic Research Promotion Fund, Grant No. M01-2003-000-20144-0).

**Supporting Information Available:** Experimental details for the preparation of **I**, **II**, **III**, and **IV** and their <sup>1</sup>H NMR spectra; <sup>13</sup>C NMR results of **I**; procedures for DLS, NMR, TEM, and MALDI-TOF MS measurements and catalytic tests, UV–vis spectra of ninhydrin and ZnTPP tests; DLS particle size distributions, and surfactant packing calculation. This material is available free of charge via the Internet at <http://pubs.acs.org>.

## References

- Woolley, K. L. *J. Polym. Sci. Part A: Polym. Chem.* **2000**, *38*, 1397–1407.
- Perkins, K. K.; Turner, J. L.; Woolley, K. L.; Mann, S. *Nano Lett.* **2005**, *5*, 1457–1461.
- (a) Sanji, T.; Ogawa, Y.; Nakatsuka, Y.; Tanaka, M.; Sakurai, H. *Chem. Lett.* **2003**, *32*, 980–981. (b) Liu, S.; Weaver, J. V. M.; Save, M.; Armes, S. P. *Langmuir* **2002**, *18*, 8350–8357.
- (a) Soppimath, K. S.; Tan, D. C.-W.; Yang, Y.-Y. *Adv. Mater.* **2005**, *17*, 318–323. (b) Rösler, A.; Vandermeulen, G. W. M.; Klok, H.-A. *Adv. Drug Delivery Rev.* **2001**, *53*, 95–108.
- Huang, H.; Rensen, E. E.; Kowalewski, T.; Woolley, K. L. *J. Am. Chem. Soc.* **1999**, *121*, 3805–3806.
- Sanji, T.; Nakatsuka, Y.; Ohnishi, S.; Sakurai, H. *Macromolecules* **2000**, *33*, 8524–8526.
- Dhas, N. A.; Suslick, K. S. *J. Am. Chem. Soc.* **2005**, *127*, 2368–2369.
- Bégu, S.; Durand, R.; Lerner, D. A.; Charnay, C.; Tourné-Péteilh, C.; Devoisselle, J. M. *Chem. Commun.* **2003**, 640–641.
- Kim, J. Y.; Yoon, S. B.; Yu, J.-S. *Chem. Commun.* **2003**, 790–791.
- Paleos, C. M.; Malliaris, A. J. *Macromol. Sci. Rev. Macromol. Chem. Phys.* **1988**, *C28*, 403–419.
- Aliev, K. V.; Ringdorf, H.; Schlarb, B.; Leister, K. H. *Macromol. Chem. Rapid Commun.* **1984**, *5*, 345–352.
- Antesberger, J.; Cave, G. W. V.; Ferrarelli, M. C.; Heaven, M. W.; Raston, C. L.; Atwood, J. L. *Chem. Commun.* **2005**, 892–894.
- Leung, D. H.; Fiedler, D.; Bergman, R. G.; Raymond, K. N. *Angew. Chem., Int. Ed.* **2004**, *43*, 963–966.
- Oh, S.-K.; Niu, Y.; Crooks, R. M. *Langmuir* **2005**, *21*, 10209–10213.
- Katz, A.; Davis, M. E. *Nature* **2000**, *403*, 286–289.
- Sarin, V. K.; Kent, S. B. H.; Tam, J. P.; Merrifield, R. B. *Anal. Biochem.* **1981**, *117*, 147–157.
- Pedersen, K. J. *J. Am. Chem. Soc.* **1929**, *51*, 2098–2107.

JA057092I